Electronic Supplementary Information

Template Directed Strategy of Green Energetic Metal-Organic Frameworks for Enhancing Oxygen Balance and Near Infrared Laser Initiation

Ruibing Lv,[a] Guangli Wang,[a] Fangbao Jiao,[a] Zhenghang Luo,[a] Yujie Song,[a] Wentao Wang,*[b] and Qi Zhang*[a]

[a] Institute of Chemical Materials, China Academy of Engineering Physics (CAEP), Mianyang 621900, P. R. China.

[b] Dalian Institute of Chemical Physics, Chinese Academy of Sciences, Dalian 116023, P. R. China.

*Corresponding author

Email address: jackzhang531@ caep.cn (Q. Zhang)

Table of Contents

1. Experimental Section

Caution! Some of the raw materials and all products introduced in this study are energetic materials with potential explosion hazards. Although no explosion occurred in our experiments, protective measures such as masks, goggles, protective clothing, gloves, etc. must be taken. All energetic compounds should be stored in a cool and dark place. No impact, friction or sparks are allowed.

General Information: Elemental analyses (C, H, and N) were carried out using the Vario EL III CHNOS device. Thermal stability analysis was carried out using a TG-DSC Mettler Toledo calorimeter equipped with an auto-cooling accessory. The impact and friction sensitivities were obtained by using a standard BAM Fall hammer and a BAM friction tester. The electrostatic potentials (ESPs) were obtained by using Multiwfn 3.8 software based on the calculation results via the Gaussian 16 program using B3LYP/6-311g** level, and analyzed via Visual Molecular Dynamics (VMD, version 1.9.3) program.

Synthesis of 4,4'-azo-1,2,4-triazole (ATRZ): Sodium dichloroisocyanurate (20.12 g, 96 mmol) was dissolved in 200 mL of deionized water at room temperature with stirring until complete dissolution. Subsequently, 10 mL of acetic acid was added, and the mixture was vigorously stirred at room temperature for 4 hours, maintaining the reaction temperature below 10 °C using an ice bath. Separately, 4-amino-1,2,4-triazole (10.1 g, 120 mmol) was dissolved in 10 mL of water and added to the reaction mixture. Stirring was continued for an additional 5 hours to ensure completion of the reaction. The reaction mixture was then filtered, and the solid obtained was dissolved in 300 mL of deionized water by boiling. After cooling for 3 hours, the solution was filtered again to isolate needle-shaped crystals of ATRZ. Yield: 5.12 g, 52%. FTIR (KBr, ν/cm^{-1}): 3115, 2946, 2656, 1736, 1492, 1369, 1317, 1180, 1036, 930, 886, 859, 690, 620, 544. Elemental analysis for $C_4H_4N_8$ (164.13 g mol^{-1}): calcd: C 29.27, H 2.46, N 68.27; found: C 29.18, H 2.59, N 68.23.

Synthesis of $[Ag(ATRZ)(DN)]_n$ (CMOF-1): ATRZ (3 mmol, 0.49 g) and Ammonium dinitramide aqueous solution (75.32%, 0.5 g, 3 mmol) were added to 15 mL of deionized water, heated to 80 °C and stirred until dissolved. Then, $AgNO_3$ aqueous solute on (1M, 3 mL) was added dropwise to the reaction system, and a large amount of white precipitate was immediately precipitated. The product was collected by filtration, washed with deionized water and ethanol, and finally dried in air to yield CMOF-1 (1.10 g, 97.0%). Vacuum distillation of the filtrate resulted in 0.22 g of solid NH_4NO_3. FTIR (KBr, ν/cm^{-1}): 3115, 1516,

1484, 1421, 1368, 1322, 1177, 1031, 1007, 873, 816, 755, 670, 621, 542. Elemental analysis for $C_4H_4AgN_{11}O_4$ (378.02 g mol^{-1}): calcd: C 12.71, H 1.07, N 40.76; found: C 12.63, H 1.15, N 40.66.

2. FTIR spectroscopy

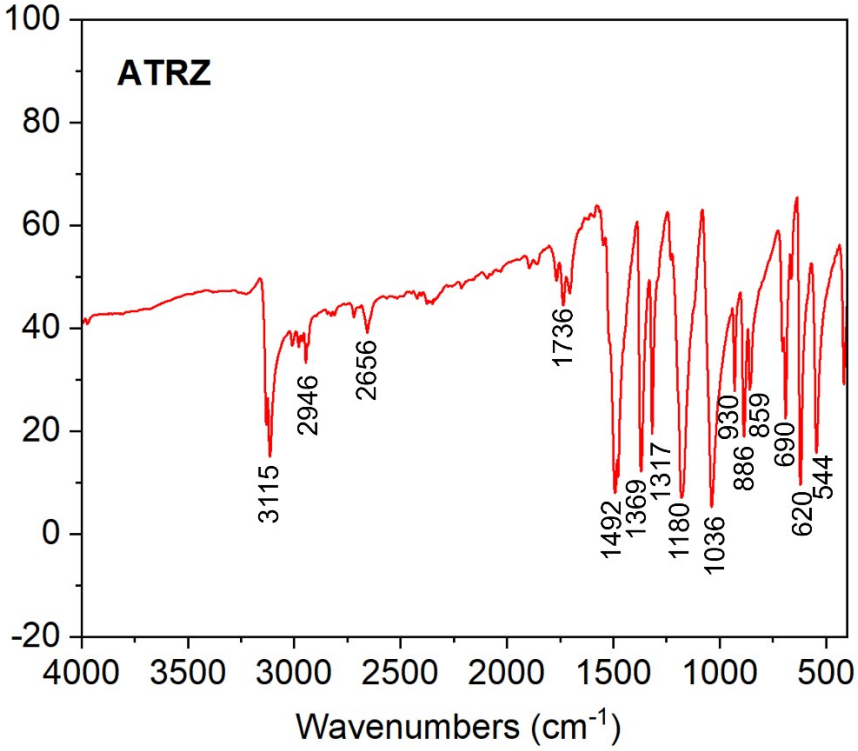

Fig. S1 FTIR Curve of 4,4'-azo-1,2,4-triazole (ATRZ).

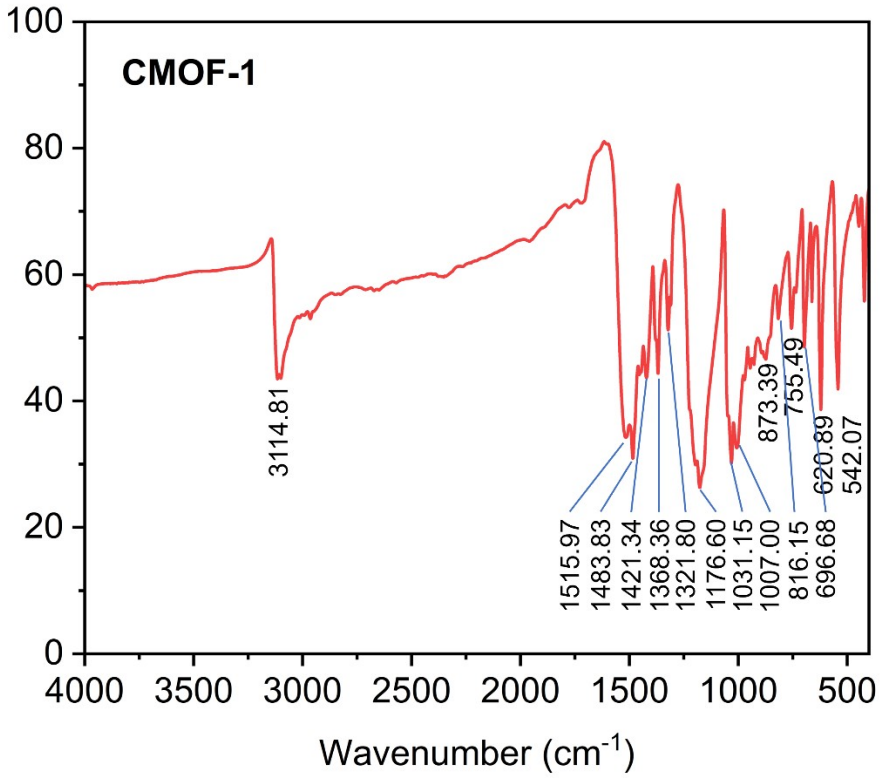

Fig. S2 FTIR Curve of $[Ag(ATRZ)(DN)]_n$ (CMOF-1).

3. Characterization of ligand ATRZ

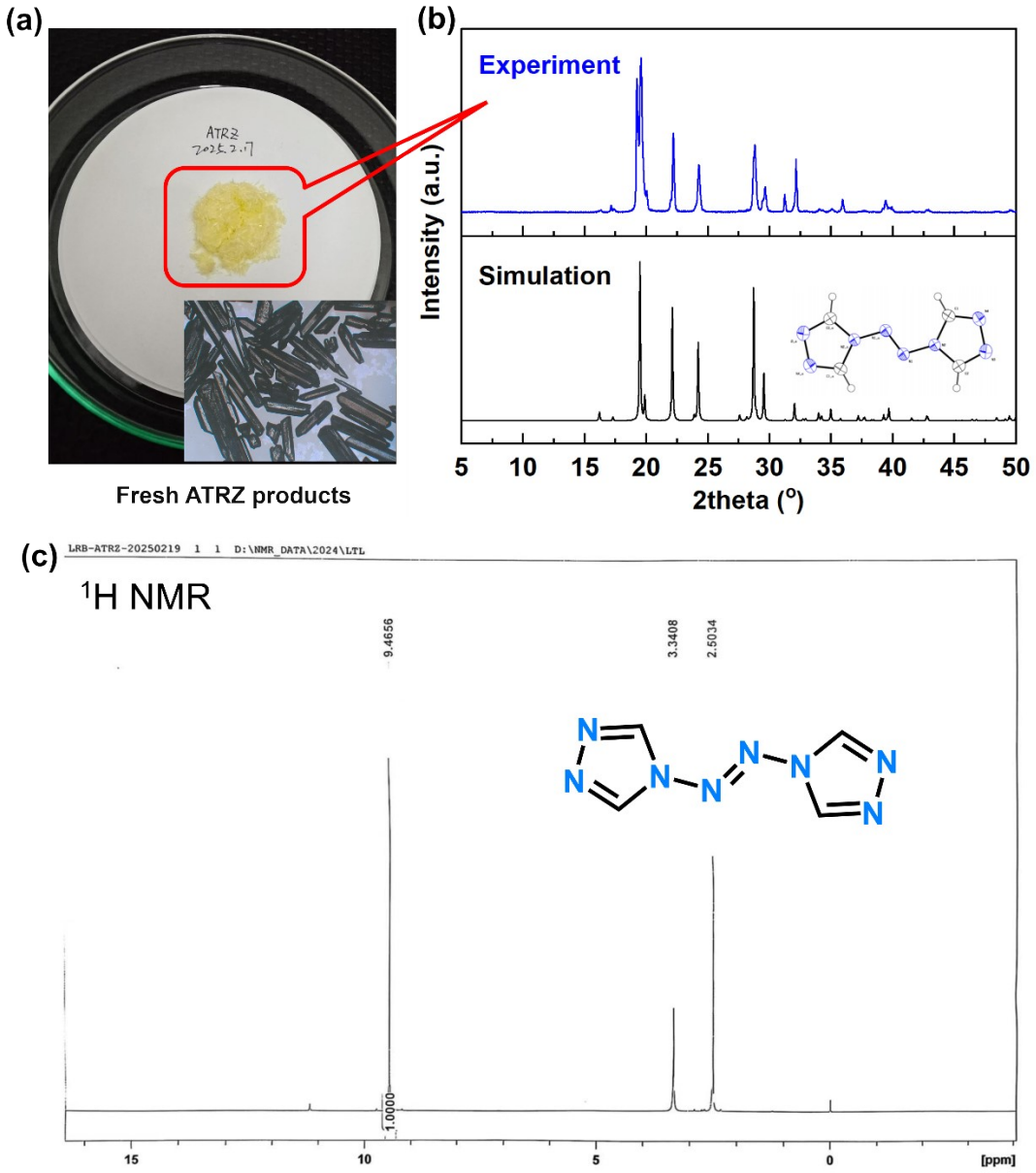

Fig. S3 (a) Optical microscope photos, (b)powder X-ray diffraction, and (c) ^{1}H NMR spectrum of ligand ATRZ**.**

4. Optical microscope photos

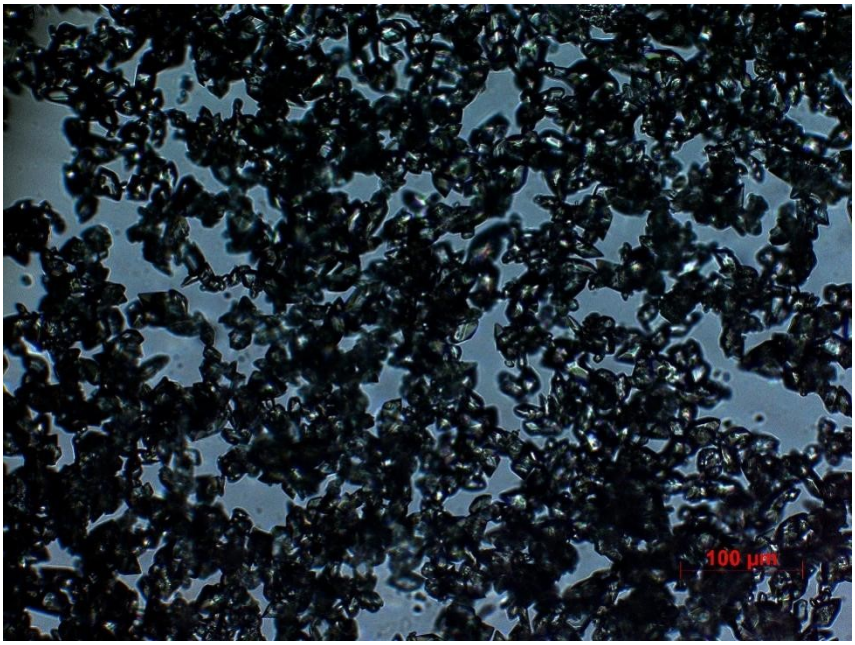

Fig. S4 (a) Optical microscope photo of CMOF-1a**.**

Fig. S5 (a) Optical microscope photo of CMOF-1b**.**

5. X-ray Crystallography

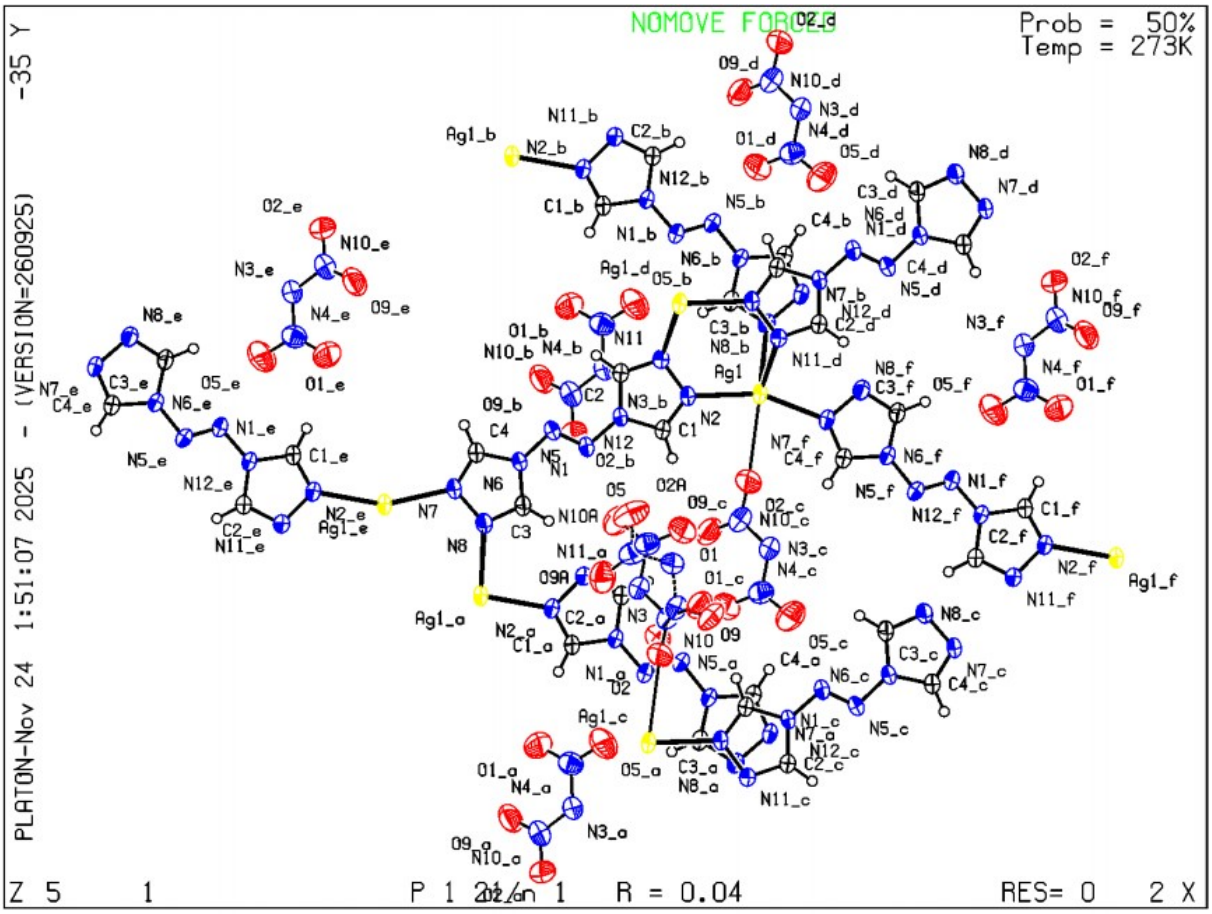

Fig. S6 The crystal structure of $[Ag(ATRZ)(DN)]_n$ (CMOF-1).

Table S1. Crystal data and structure refinement for $[Ag(ATRZ)(DN)]_n$ (CMOF-1).

Compounds	$[Ag(ATRZ)(DN)]_n$ (CMOF-1)
CCDC number	2479315
Empirical formula	$C_4H_4AgN_{11}O_4$
Formula weight	378.05
Temperature/K	273.15
Crystal system	monoclinic
Space group	$P2_1/n$
a/Å	7.052(3)
b/Å	13.474(6)
c/Å	11.786(5)
α/°	90
β/°	99.362(15)
γ/°	90
Volume/Å^3	1105.0(8)
Z	4
ρ_{calc}g/cm^3	2.272
μ/mm^{-1}	1.866
F(000)	736.0

Crystal size/mm^3	0.22 × 0.2 × 0.18
Radiation	MoKα (λ = 0.71073)
2Θ range for data collection/°	6.04 to 61.2
Index ranges	-10 ≤ h ≤ 8, -19 ≤ k ≤ 17, -15 ≤ l ≤ 16
Reflections collected	21093
Independent reflections	3377 [R_{int} = 0.1183, R_{sigma} = 0.0866]
Data/restraints/parameters	3377/262/245
Goodness-of-fit on F^2	1.005
Final R indexes [I>=2σ (I)]	R_1 = 0.0398, wR_2 = 0.0638
Final R indexes [all data]	R_1 = 0.1060, wR_2 = 0.0752
Largest diff. peak/hole / e Å^{-3}	0.39/-0.48

Table S2. Selected bond lengths [Å] for $[Ag(ATRZ)(BrO_3)]_n$ (CMOF-1).

Atom	Atom	Length/Å	Atom	Atom	Length/Å
Ag1	N7^1	2.211(2)	N11	Ag1^2	2.560(3)
Ag1	N2	2.216(3)	N11	C2	1.299(4)
Ag1	N11^2	2.560(3)	N8	Ag1^5	2.542(3)
Ag1	N8^3	2.542(3)	N8	C3	1.298(4)
N12	N1	1.383(3)	O5	N4	1.232(9)
N12	C2	1.359(4)	N10	O9	1.213(9)
N12	C1	1.360(4)	N10	O2	1.201(9)
N7	Ag1^4	2.211(2)	N10	N3	1.373(12)
N7	N8	1.407(3)	N4	N3	1.377(11)
N7	C4	1.297(4)	N4	O1	1.197(7)
N1	N5	1.238(3)	N3A	N4A	1.361(14)
N5	N6	1.385(3)	N3A	N10A	1.391(14)
N2	N11	1.403(3)	O5A	N4A	1.280(14)
N2	C1	1.286(4)	N4A	O1A	1.256(13)
N6	C4	1.357(3)	N10A	O9A	1.208(11)
N6	C3	1.358(4)	N10A	O2A	1.191(16)

Table S3. Selected bond Angles [°] for $[Ag(ATRZ)(BrO_3)]_n$ (CMOF-1).

Atom	Atom	Atom	Angle/°	Atom	Atom	Atom	Angle/°
N7^1	Ag1	N2	156.79(10)	C2	N11	N2	107.2(2)
N7^1	Ag1	N11^2	97.10(9)	N7	N8	Ag1^5	133.12(19)
N7^1	Ag1	N8^3	99.23(9)	C3	N8	Ag1^5	113.1(2)
N2	Ag1	N11^2	100.94(9)	C3	N8	N7	106.4(3)
N2	Ag1	N8^3	98.55(9)	N7	C4	N6	109.1(3)
N8^3	Ag1	N11^2	78.60(9)	N11	C2	N12	109.1(3)
C2	N12	N1	131.8(2)	N2	C1	N12	109.3(3)
C2	N12	C1	106.6(2)	N8	C3	N6	110.1(3)
C1	N12	N1	121.6(2)	O9	N10	N3	122.4(8)
N8	N7	Ag1^4	118.72(19)	O2	N10	O9	122.0(12)
C4	N7	Ag1^4	132.6(2)	O2	N10	N3	115.5(8)

C4	N7	N8	108.0(2)	O5	N4	N3	114.4(7)
N5	N1	N12	110.4(2)	O1	N4	O5	122.5(11)
N1	N5	N6	108.3(2)	O1	N4	N3	122.6(7)
N11	N2	Ag1	124.46(18)	N10	N3	N4	118.3(6)
C1	N2	Ag1	127.8(2)	N4A	N3A	N10A	109.9(9)
C1	N2	N11	107.7(2)	O5A	N4A	N3A	108.6(9)
C4	N6	N5	124.2(3)	O1A	N4A	N3A	129.8(13)
C4	N6	C3	106.4(2)	O1A	N4A	O5A	120.1(12)
C3	N6	N5	129.3(2)	O9A	N10A	N3A	126.6(10)
N2	N11	Ag1[2]	120.08(18)	O2A	N10A	N3A	109.0(12)
C2	N11	Ag1[2]	114.7(2)	O2A	N10A	O9A	123.6(13)

Table S4. Selected torsion Angles [°] for $[Ag(ATRZ)(BrO_3)]_n$ (CMOF-1).

Atom	**Atom**	**Atom**	**Atom**	**Angle/°**	**Atom**	**Atom**	**Atom**	**Atom**	**Angle/°**
Ag1[1]	N7	N8	Ag1[2]	40.2(3)	N8[5]	Ag1	N2	N11	-38.7(2)
Ag1[1]	N7	N8	C3	-173.0(2)	N8[5]	Ag1	N2	C1	138.6(3)
Ag1[1]	N7	C4	N6	171.6(2)	N8	N7	C4	N6	1.1(4)
Ag1	N2	N11	Ag1[3]	-48.4(3)	C4	N7	N8	Ag1[2]	-147.8(2)
Ag1	N2	N11	C2	178.2(2)	C4	N7	N8	C3	-1.0(4)
Ag1	N2	C1	N12	-178.39(19)	C4	N6	C3	N8	0.2(4)
Ag1[3]	N11	C2	N12	-136.2(2)	C2	N12	N1	N5	-16.0(4)
Ag1[2]	N8	C3	N6	154.7(2)	C2	N12	C1	N2	0.7(4)
N12	N1	N5	N6	-179.1(2)	C1	N12	N1	N5	164.4(3)
N7[4]	Ag1	N2	N11	-178.4(2)	C1	N12	C2	N11	-0.4(3)
N7[4]	Ag1	N2	C1	-1.1(5)	C1	N2	N11	Ag1[3]	133.8(2)
N7	N8	C3	N6	0.5(4)	C1	N2	N11	C2	0.5(4)
N1	N12	C2	N11	180.0(3)	C3	N6	C4	N7	-0.8(4)
N1	N12	C1	N2	-179.6(3)	O5	N4	N3	N10	-173.7(18)
N1	N5	N6	C4	-164.5(3)	O9	N10	N3	N4	5(2)
N1	N5	N6	C3	16.7(4)	O2	N10	N3	N4	-178.2(15)
N5	N6	C4	N7	-179.8(3)	O1	N4	N3	N10	14.7(18)
N5	N6	C3	N8	179.1(3)	N4A	N3A	N10A	O9A	14.5(17)
N2	N11	C2	N12	0.0(3)	N4A	N3A	N10A	O2A	-175.7(16)

6. TG-DSC curves

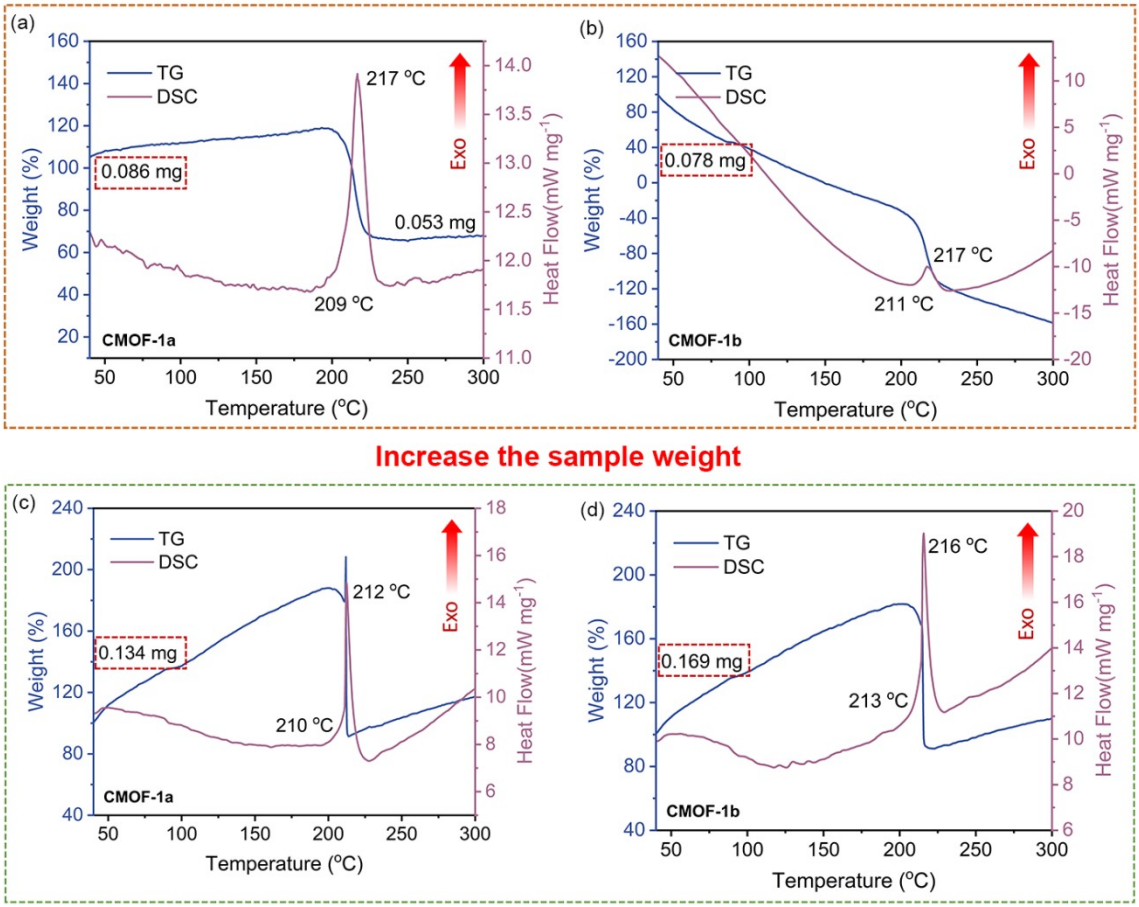

Fig. S7 (a) The TG-DSC curve of CMOF-1a with an initial weight of 0.086 mg. (b) The TG-DSC curve of CMOF-1b with an initial weight of 0.078 mg. (c) The TG-DSC curve of CMOF-1a with an initial weight of 0.134 mg. (d) The TG-DSC curve of CMOF-1b with an initial weight of 0.169 mg.

7. Vary temperature X-ray Diffraction

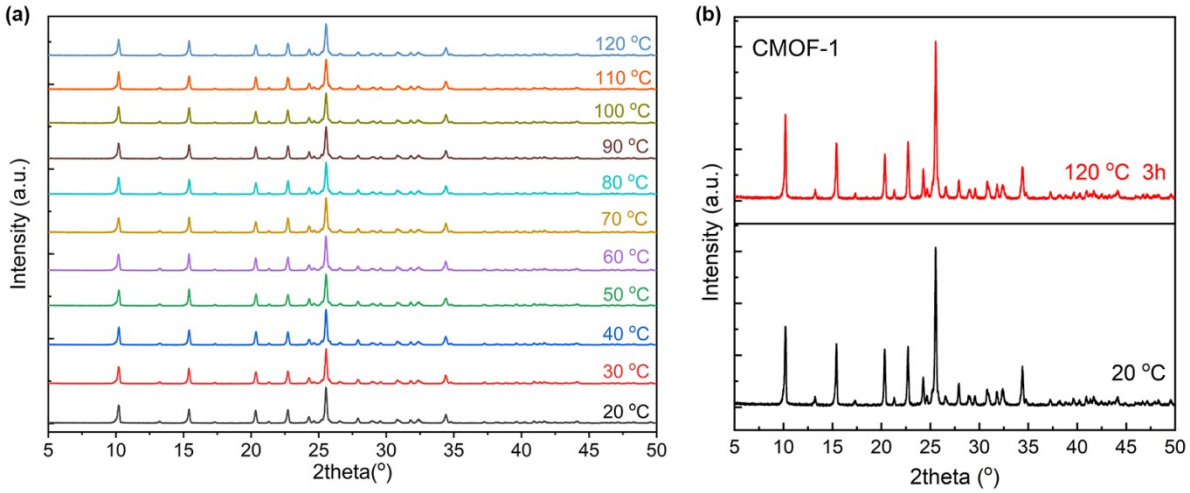

Fig. S8 Vary temperature PXRD curves of CMOF-1a in air atmosphere.

8. Pressure-time relationship of detonation

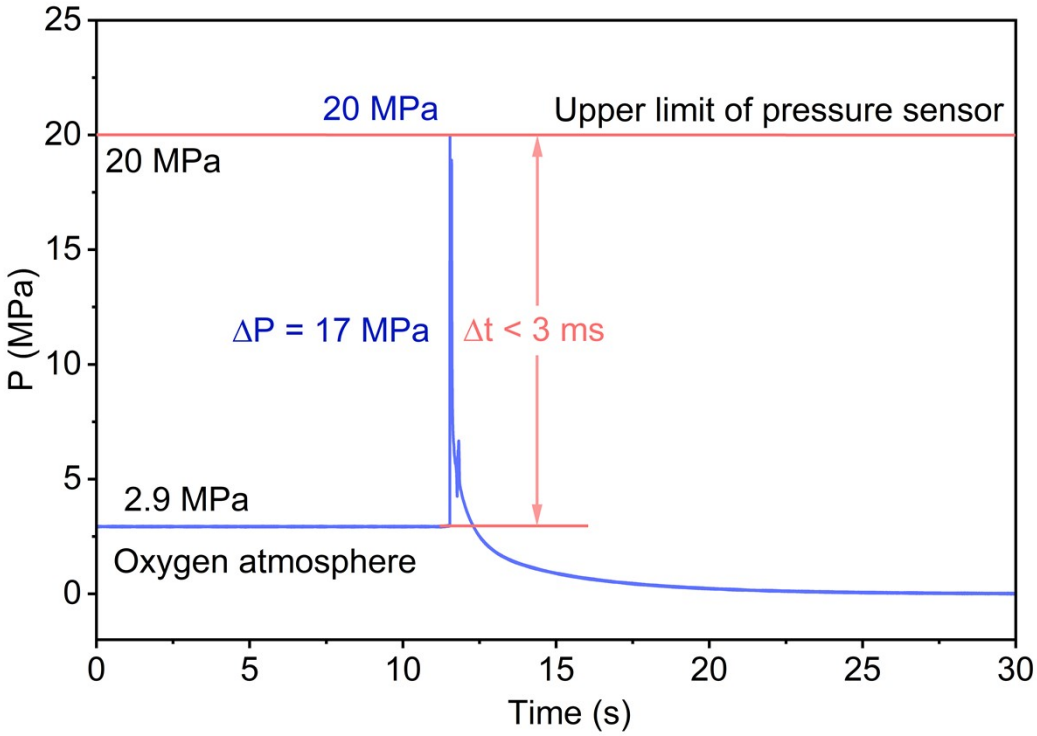

Fig. S9 Pressure-time curve of detonation of CMOF-1 in oxygen atmosphere.